Detailed Analysis of Shrinkage and Creep Effect of Concrete in Prestressed Box Girder Bridge

Donglian Tan, Wenyuan Ding, Yue Zhao, and Chuqin Yan

Abstract For a 60 m prestressed concrete box girder bridge using structural analysis software as ANSYS and MIDAS/civil, combined with several creep prediction models, a reasonable creep prediction model has been obtained. Considering the influence of prestressed tendon relaxation on the shrinkage and creep of concrete, a refined finite element model is established for numerical analysis and compared with the experimental data. The comparison results show that the calculated value of the refined finite element model with reasonable prediction models and considering the effect of prestress relaxation is closer to the measured value. Finally, the finite element model of solid elements considering the effect of prestress relaxation with the GL2000 creep prediction model is used to analyze the shrinkage and creep effect of a prestressed concrete continuous rigid frame bridge.

Keywords Shrinkage and Creep · Prediction Models · Prestressed Concrete Box Girder · Continuous Rigid Frame Bridge · Accurate Analysis

1 Introduction

Prestressed concrete box girder has been widely used in bridges for its advantages of large structural stiffness, small deformation and beautiful shape. However, the inherent performance of concrete as shrinkage and creep has obvious impact on bridge deflection. It will lead to the bridge alignment cannot reach the expected design alignment. The shrinkage and creep of concrete has time-varying characteristics. Its laws are complex and changeable. It is one of the most uncertain characteristics of concrete. At present, there are many creep prediction models. The calculation results of various models are quite different. There are many factors influencing the shrinkage and creep of concrete. In this paper, combined with the measured values of concrete shrinkage and creep deformation of a 60 m prestressed concrete box

D. Tan (✉) · W. Ding · Y. Zhao · C. Yan
School of Railway Transportation, Shanghai Institute of Technology, 100 Haiquan Road, Fengxian District, Shanghai, China
e-mail: tdl021@126.com

G. Feng (ed.), *Proceedings of the 9th International Conference on Civil Engineering*, Lecture Notes in Civil Engineering 327,
https://doi.org/10.1007/978-981-99-2532-2_8

girder bridge, the refined analysis method of shrinkage and creep deformation of a prestressed concrete box girder bridge is studied. Then, the concrete shrinkage and creep effect of a prestressed concrete continuous rigid frame bridge is analyzed using the method proposed in this paper.

2 Prediction Model of Concrete Shrinkage and Creep

Based on the analysis of the establishment mechanism of the concrete creep prediction model, the creep prediction model can be divided into two categories.

One is to construct prediction formulas such as hyperbolic function, power function and exponential function by observing and studying the distribution phenomenon of many experimental data. Many prediction models according to this method have been established in the early stage. The most influential one is the hyperbolic power function prediction model proposed by Professor Ross in 1937, which was introduced by ACI in 1970. It was adopted by the 209 Committee after revision. Up to now, the ACI 209 committee still maintains the framework of this prediction model, only modifying the parameters.

The other is to establish the framework of a prediction model based on theoretical analysis and determine parameters by regression based on experimental data. This kind of model generally has a clear physical meaning and develops and improves with the development of theory. CEB-FIP (1978), BP-KX and B3 models are all such models. CEB-FIP (1990) creep prediction model has made a great adjustment to CEB-FIP (1978) model, from the form of continuous addition to the form of continuous multiplication. From the form of the formula, it is closer to the former one.

For the establishment mechanism of concrete shrinkage prediction models, almost all prediction models are constructed according to hyperbolic function or hyperbolic power function, and the fitting parameters of the models are adjusted through experiments and theoretical analysis. From the current research reports, no matter which form of prediction model is used, if the parameters are accurate and appropriate, the prediction results are in good agreement with the actual situation. The following four main forecasting models are introduced, which are CEB-FIP series model, ACI 209 model, B3 model and GL2000 model.

2.1 CEB-FIP Series Forecasting Model

The CEB-FIP (1978) model was jointly launched by CEB and FIP in 1978. In this model, the formula of creep coefficient is expressed in the form of continuous addition. Creep is composed of irrecoverable creep and recoverable creep. Irrecoverable creep is divided into initial creep and lag creep under loading. The shrinkage function of CEB-FIP (1978) model is expressed as the product of basic shrinkage coefficient and shrinkage time function.

CEB-FIP (1990) model was put forward by CEB-FIP organization in 1990. The model does not specifically distinguish various types of creep. The formula is expressed in the form of continuous multiplication. The variation law of creep coefficient with time is fitted as a hyperbolic power function. The formula is obtained by multiplying three correction coefficients.

$$\varphi(t,\tau) = \varphi_0\beta_c(t,\tau) = \varphi_{RH}\beta(f_{cm})\beta(\tau)\beta_c(t-\tau) \quad (1)$$

where, φ_0 is the nominal creep coefficient; φ_{RH} is the correction factor of environmental relative humidity; $\beta(f_{cm})$ is the concrete strength correction factor; $\beta(\tau)$ is the loading age correction factor; $\beta_c(t-\tau)$ is the creep process time function.

The contraction function of CEB-FIP (1990) is as follows:

$$\varepsilon_{cs}(t,t_s) = \varepsilon_{cs0}\beta_s(t-t_s) = \varepsilon_s(f_{cm})\beta_{RH}\beta_s(t-t_s) \quad (2)$$

where, ε_{cs0} is the nominal shrinkage factor, $\varepsilon_s(f_{cm})$ is the concrete strength correction factor, β_{RH} is the correction factor of environmental relative humidity, $\beta_s(t-t_s)$ is the shrink process time function.

In the CEB-FIP (1990) model, the effects of loading age, environmental relative humidity, member size and concrete strength are considered in creep, which greatly improves CEB-FIP (1978) model.

2.2 ACI209 Series Forecasting Model

ACI209 is a prediction model recommended by American Concrete Institute (ACI), which is adopted by American state specifications, and is also used as a reference comparison standard for Canada, New Zealand, Australia and some Latin American countries.

ACI209 Committee has launched ACI 209–1978 model, ACI 209–1982 model, ACI 209r-1992 model [9]. The creep coefficient of ACI 209 series model is expressed as follows:

$$\varphi(t,\tau) = \varphi(\infty)\frac{(t-\tau)^{0.6}}{10+(t-\tau)^{0.6}} \quad (3)$$

where, $\varphi(\infty)$ is the ultimate value of creep coefficient, $\varphi(\infty) = 2.35\gamma_c$, 2.35 is the ultimate value of creep coefficient under standard state, γ_c is the correction coefficient of various factors affecting creep in deviating from the standard state.

The contraction function of ACI 209 mode is as follows:

$$\varepsilon_{\rm sh}(t, t_0) = \frac{t - t_0}{H + t - t_0}\varepsilon_{\rm sh\infty} \tag{4}$$

where, $\varepsilon_{\rm sh}(t, t_0)$ is Shrinkage strain at t; $\varepsilon_{\rm sh\infty}$ is the ultimate shrinkage strain, $\varepsilon_{\rm sh\infty} = 780 \times 10^{-6}\gamma_{sh}$, 780×10^{-6} is the ultimate value of shrinkage strain under standard conditions, γ_{sh} is the correction coefficient of each influencing factor when it deviates from the standard state; t_0 is the age of completion of maintenance; H is the coefficient related to maintenance.

ACI 209 series model considers that the size of the component has no effect on the ultimate value of shrinkage and creep, which is inconsistent with the test results. Moreover, the parameters of the shrinkage and creep time process function are taken as constants in this series of models, which cannot reflect the development law of shrinkage and creep of concrete with different strength grades over time. Therefore, ACI 209 series model needs to be further revised.

2.3 B3 Prediction Model

B3 prediction model, which is simpler and more theoretical, was proposed in 1997 by Professor Z.P.Bažant on the basis of BP model (proposed in 1978) and BP-KX model (proposed in 1991). B3 model is a shrinkage creep prediction model recommended by RILEM. The B3 model of concrete creep is established based on the solidification theory of concrete, which combines the elastic theory, viscoelastic theory and rheological theory to simulate the new theory that the macroscopic physical and mechanical properties of concrete change with time due to the hydration of cement and the increase of solid phase. It holds that the dependence of macroscopic material parameters of concrete on time is the result of the increasing volume of viscous phase and viscoelastic phase of concrete material, while the mechanical properties, elastic phase volume and non-bearing phase volume (such as pores, colloids, water, etc.) are constantly changing.

The creep coefficient expression of B3 prediction model:

$$\varphi(t, \tau) = \frac{J(t, \tau) - 1/E(\tau)}{1/E(\tau)} = E(\tau)J(t, \tau) - 1 \tag{5}$$

where, $J(t, \tau)$ is a creep function; $E(\tau)$ is the elastic modulus of concrete at τ.

The contraction function expression of B3 prediction mode is as follows:

$$\varepsilon_{\rm sh}(t, \tau) = \varepsilon_{\rm sh\infty}k_{\rm h}S(t) \tag{6}$$

where, $\varepsilon_{\rm sh\infty}$ is the ultimate shrinkage strain, $k_{\rm h}$ is the humidity correction factor, when $h \leq 0.98$, $k_h = 1 - h^3$; when $h = 1.00$, $k_h = -0.2$; when $0.98 \leq h \leq 1.00$, it is obtained by linear interpolation; $S(t)$ is the time process function.

B3 prediction model is a semiempirical and semi theoretical formula. Bezant pointed out that in order to improve the theoretical and prediction accuracy of the model, the calculation formula of various material parameters should also be established on a certain theoretical basis, and the research in this field needs to be further carried out.

The accuracy of B3 prediction model is limited by many conditions. Compared with CEB-FIP model and ACI 209 mode, B3 mode needs more parameters and more calculation.

2.4 GL2000 Prediction Model

Based on some criteria that should be satisfied by the shrinkage creep prediction model adopted by ACI 209 Committee in 1999, Gardner and Lockman revised the atlanta97 model (proposed by Gardner and Zhao in 1993) and proposed GL2000 model. The model can be applied to high strength concrete, and the influence of concrete drying before loading on creep deformation after loading is considered by a single item. The GL2000 model is described as follows:

Creep Coefficient:

$$\varphi_{28} = \Phi(t_c)\left\{\begin{array}{l} 2\left[\dfrac{(t-t_0)^{0.3}}{(t-t_0)^{0.3}+14}\right]+\left(\dfrac{7}{t_0}\right)^{\frac{1}{2}}\left[\dfrac{t-t_0}{t-t_0+7}\right]^{\frac{1}{2}} \\ +2.5\left(1-1.086h^2\right)\left[\dfrac{t-t_0}{t-t_0+0.15\left(\frac{V}{S}\right)^2}\right]^{\frac{1}{2}} \end{array}\right\} \tag{7}$$

$$\Phi(t_c) = \begin{cases} \left[1-\left(\dfrac{t-t_0}{t-t_0+0.15\left(\frac{V}{S}\right)^2}\right)^{\frac{1}{2}}\right]^{\frac{1}{2}}, & t_0 > t_c \\ 1, & t_0 = t_c \end{cases} \tag{8}$$

where, φ_{28} is the creep coefficient of concrete at 28 days age. t is the calculation concrete age. t_0 is the loading age of concrete. t_c is the age of concrete at the beginning of drying. V/S is the ratio of volume to surface area of concrete components.

Shrinkage strain:

$$\varepsilon_{sh} = \varepsilon_{shu}\beta(h)\beta(t) \tag{9}$$

$$\beta(h) = 1 - 1.18h^4 \tag{10}$$

$$\varepsilon_{shu} = 900k\left(\frac{30}{f_{cm28}}\right)^{\frac{1}{2}} \times 10^{-6} \tag{11}$$

$$\beta(t) = \left(\frac{t - t_c}{t - t_c + 0.15\left(\frac{V}{S}\right)^2} \right)^{\frac{1}{2}} \tag{12}$$

where, h is the environmental relative humidity. t is the calculation concrete age. t_0 is the loading age of concrete. t_c is the age of concrete at the beginning of drying. k shrinkage coefficient which depends on cement type. V/S is the ratio of volume to surface area of concrete components. f_{cm28} is the average cube compressive strength of concrete at 28 days of age.

3 Comparison of Prediction Models

3.1 Calculation Method

Midas /civil has two methods for creep analysis, one is to directly define the creep coefficient of each stage of the element, and the other is to use the creep function to calculate by integral. The influence of early shrinkage and creep of concrete in construction stage can be considered in the software. Moreover, the software provides the calculation standards of many countries, which can fit the creep coefficient and shrinkage strain conveniently [4-10].

3.2 Finite Element Model

In this section, in order to compare CEB-FIP, ACI209 and GL2000 prediction models, the finite element model of the test beam is established by the bridge structure analysis program Midas for numerical simulation analysis. The calculation model is shown in Fig. 1.

The box girder is made of C55 concrete. According to the material property test results of concrete specimens, the elastic modulus is 4.65×10^4 MPa, and the 28-day cube compressive strength is 65.6 MPa; the Poisson's ratio of concrete material is 0.2, and the bulk density is $26.5 kn/m^3$.

The prestressed steel specific parameters are shown in Table 1.

According to the measured results, the influence coefficient K of local deviation of prestressed pipe is 0.001454, and the friction coefficient μ of pipeline is 0.1470.

Fig. 1 Finite element model of test beam

Table 1 Mechanical property index of prestressed steel strand

Elastic modulus (MPa)	1.95×10^5
f_{ptk} (MPa)	1860
Nominal diameter(mm)	15.2
Nominal section area(mm^2)	139
Nominal mass(kg/m)	1.101
Relaxation rate	2.5%
Tension control stress (MPa)	1395

3.3 Comparison of Calculated Results and Measured Results

The creep deflections of aci209, CEB-FIP and gl2000 are calculated by using the above finite element models and compared with the measured results. The results are shown in Fig. 2.

From the comparison chart, it can be seen that the calculation results of GL2000 creep prediction model are close to the measured values, except that the difference of some measuring points reach 18%, the rest are less than 10%. Therefore, the following analysis uses GL2000 prediction model.

4 Fine Analysis of Shrinkage Creep Deformation of Concrete Box Girder

According to the comparison results in Sect. 2, the calculation results of GL2000 prediction model are the closest to the measured values. The GL2000 concrete shrinkage and creep prediction model is used for the refined analysis of the shrinkage and creep deformation of the concrete box girder. MIDAS/civil finite element model using three-dimensional beam element, ANSYS solid model without considering the influence of prestressed tendon relaxation, and ANSYS solid model considering the influence of prestressed tendon relaxation are used respectively. Three kinds of refined finite element models are analyzed and compared.

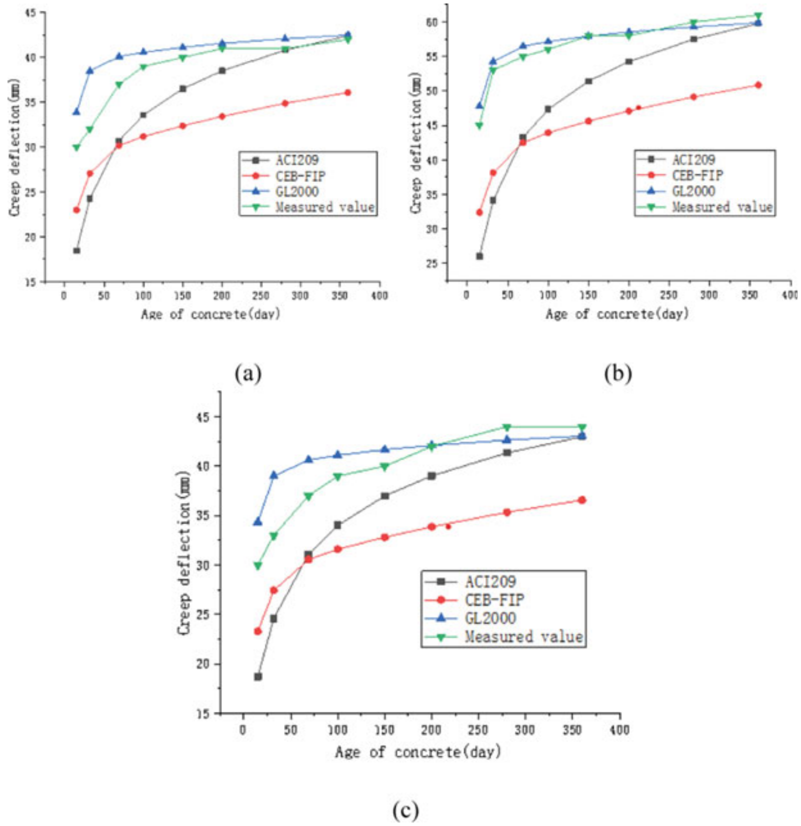

Fig. 2 Comparison between the calculated results and the measured ones **a** 1/4 span; **b** Middle span; **c** 3/4 span

4.1 MIDAS/civil Beam Element Model

The finite element model of 60 m concrete beam was set up according to the construction stage using MIDAS/civil. The finite element model is shown in Fig. 3.

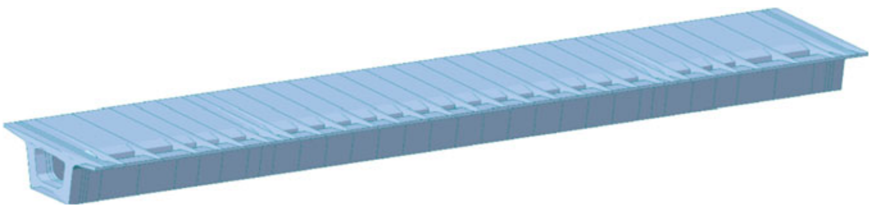

Fig. 3 Three-dimensional beam model of Midas

4.2 ANSYS Solid Model without Considering the Influence of Prestressed Tendon Relaxation

Without considering the influence of the relaxation of prestressed tendons on the shrinkage and creep, the prestress is applied with the initial strain in the deduction of prestress loss. The concrete is built with SOLID65 element, which can consider the creep of concrete. There are 2610 concrete units in the whole bridge. The prestressed reinforcement is built with link8 unit, with a total of 386 prestressed reinforcement units. In the ANSYS analysis. It is considered that the concrete does not crack and there is no sliding between the prestressed reinforcement and the concrete.

4.3 ANSYS Solid Model Considering the Influence of Prestressed Tendon Relaxation

In order to consider the influence of prestress relaxation on concrete shrinkage and creep, the time development process of prestress loss caused by prestress relaxation is considered in the analysis. Finite element models are the same as those in the previous paragraph.

4.4 Comparison of Calculated Values and Experimental Values of Three Models

The comparison between the theoretical calculation results of the three finite element models and the test results is shown in Fig. 4. Method 1 in the table refers to MIDAS/civil space beam finite element model, method 2 means ANSYS solid model without considering the effect of prestressed tendon relaxation, method 3 is ANSYS solid model considering the influence of prestressed tendon relaxation.

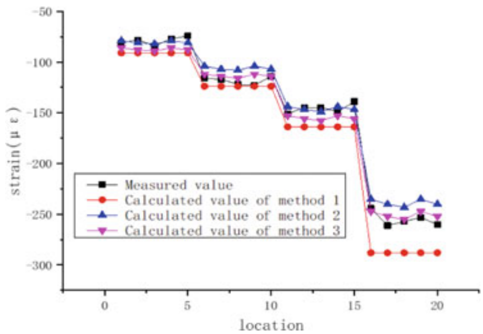

Fig. 4 Comparison of calculated and experimental values

In method 2, the restraint effect of prestressed tendons on concrete is considered, but the influence of relaxation of prestressed tendons on concrete shrinkage and creep is not considered. The prestress loss caused by relaxation of prestressed tendons is deducted at the initial time, which makes the theoretical value of initial strain of concrete less than the experimental value, so the theoretical value of strain generated by shrinkage and creep is also less than the experimental value. In method 3, not only the restraint effect of concrete is considered, but also the influence of prestress relaxation on concrete shrinkage and creep is considered. The theoretical calculation value is closest to the experimental value.

5 Detailed Analysis of a Prestressed Concrete Continuous Rigid Frame Bridge

5.1 Bridge Overview

The span layout of a bridge is 90 m + 2 × 160 m + 90 m. The beam section is single box single cell box girder. The height of the box girder is changed from 9.0 m at the root to 3.5 m in the middle of the span. The width of the top plate of the box girder is 12.0 m, the width of the bottom plate is 6.50 m. The thickness of the top plate is 0.30 m. The thickness of the bottom plate is changed from 0.32 m in the middle of the span to 1.10 m in the root according to the quadratic parabola. The thickness of webs is 0.45 m and 0.60 m respectively. The prestress of the girder includes longitudinal prestress, transverse prestress and vertical prestress.

The piers are all double thin-walled hollow piers, which are 6.5 m across the bridge and 2.5 m along the bridge. The wall thickness is 0.5 m along the bridge direction and 0.8 m in the transverse direction.

The beam is made of C50 concrete, whose elastic modulus is 3.45×10^4 MPa. The pier is made of C40 concrete, whose elastic modulus is 3.25×10^4 MPa. The high-strength relaxation steel strand is used for the longitudinal prestressing of the bridge. Its elastic modulus and the relaxation rate are 1.95×10^5 MPa and 0.3.

The bridge is in the inland cool subtropical mountain climate zone. The annual average temperature is 15.1°C. The extreme maximum temperature is 41.7°C, while the extreme minimum temperature is - 10.2°C. The annual rainfall is 800–1000 mm. The relative humidity is 0.50–0.60.

5.2 Finite Element Model

Because the bridge is a symmetrical structure, in order to improve the calculation efficiency and reduce the calculation cost, only the finite element model of half bridge is established. The treatment on the boundary is to impose longitudinal symmetric constraint on the beam section at pier. It can ensure the consistency between the results and the whole bridge model. Because the main purpose is to analyze the shrinkage and creep effect of the main girder, the pier is established by beam element. The treatment method is to set up a rigid arm to restrain the deformation of pier top and girder bottom. It ensures the deformation coordination of pier top and girder bottom.

In order to better simulate the actual internal force state of the bridge when the bridge is completed, the key construction stage of the bridge is considered by using the unit life and death function provided by ANSYS software in the solid finite element model. The key construction stages are the maximum cantilever - side span closure - bridge completion. Because the relaxation of prestress mainly occurs in the period from tension to 40 days after tension, and concrete creep develops rapidly in the early days. In order to reduce the error caused by the division of time steps, the method of first small and then long is adopted in the time step division. A total of 23 time steps are divided into a total of 4210 days.

The pre-stressed steel bars are simulated by link8 element. The area and initial strain of reinforcement are considered in the real constant of the element.

5.3 Deflection Caused by Shrinkage and Creep

Considering the influence of prestressed tendon relaxation on concrete shrinkage and creep, the deflections of the centerline of half bridge deck caused by shrinkage and creep in one year, three years and ten years are analyzed. Their results are shown in Fig. 5.

It can be seen from Fig. 5 that the deflection of girder develops rapidly within one year after the completion of the bridge, while it gradually slows down a year later. The deflection of the middle span is greater than that of the side span. In order to analyze the structural deformation caused by the relaxation of prestressed tendons

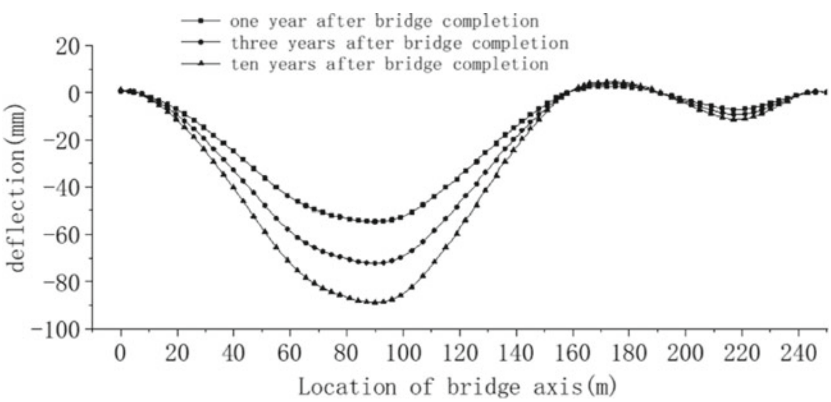

Fig. 5 Deflection by shrinkage creep (half bridge)

Table 2 Creep deformation over time (mm)

Section	Finished State	One year	Three years	Ten years
mid-span deformation of middle span	−33.4	−88.9	−102.0	−118.9
axial displacement of 1# pier top	−20.2	−76.5	−88.6	−103.8

on the shrinkage and creep of concrete, the vertical displacement in the middle span of the girder and the horizontal displacement of the pier are analyzed, as shown in Table 2.

It can be seen from the figures and tables that when considering the influence of prestressed relaxation on shrinkage and creep. Shrinkage and creep deflection of concrete in middle span is -55.5 mm in one year after completion and −68.6 mm in the third year after completion. It can be seen that the vertical displacement of the box girder due to shrinkage and creep is nearly 3 times of that at the completion time. It has reached 2 times of the completion time in one year.

5.4 *Shrinkage Creep Stress*

The shrinkage and creep stress of box roof and box floor at the time of completion, 1 year, 3 years and 10 years are shown in Fig. 6. and Fig. 7.

It can be seen from the figure that the roof stress decreases from the pier position to the middle of the span. The stress of the bottom plate increases from the support point to the middle of the span, while it decreases near the middle of the span. It is indicated that the stress change of the bottom plate is more complex. Moreover, the creep in the first year accounts for 80% of the total. Therefore, the stress state of some key sections should be accurately analyzed, such as the section at pier and mid-span section of middle span.

Because the shear stress and normal stress of the web are relatively large, the main stress state of concrete directly affects the failure mode of the structure. Therefore,

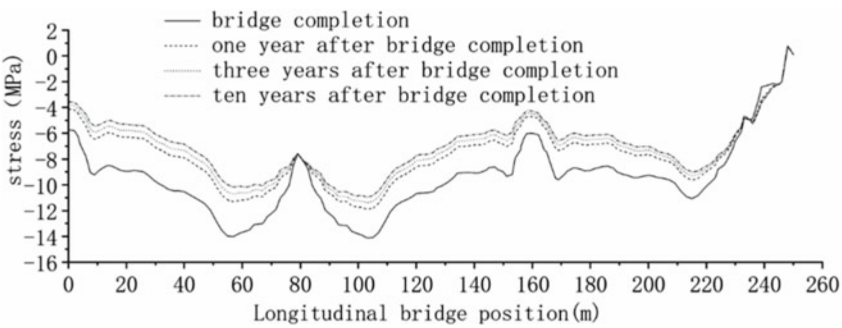

Fig. 6 Roof stress (half bridge)

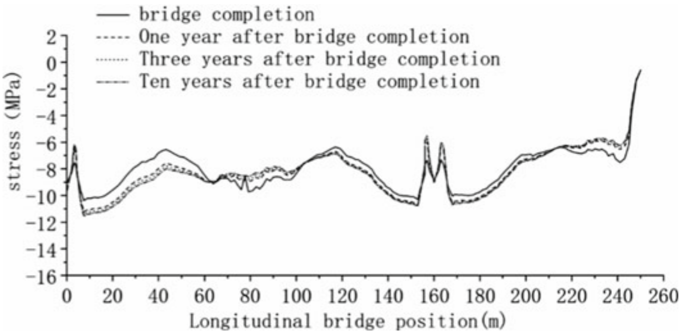

Fig. 7 Floor stress (half bridge)

it is of great significance to study the influence of concrete shrinkage and creep on the main stress of box girder web.

5.5 *Prestress Loss*

In long-span bridges, the prestress loss of different positions are quite different. The top plate steel tendons T20, web tendons W6, bottom plate steel tendons B7 and D17 of middle span closure section are selected for analysis.

In order to study the law of prestress loss, the absolute and relative values of prestress loss calculated by different calculation methods are compared, as shown in Table 3, Table 4, Table 5 and Table 6. In the table, the method I refers to the solid element model considering the effect of prestressed tendon relaxation on concrete shrinkage and creep, and the method II refers to the beam element model.

Table 3 Prestress loss of tendon T20

Method	One year		Three years		Ten years	
	value (MPa)	rate (%)	value (MPa)	rate (%)	value (MPa)	rate (%)
method I	−83.41	6.97	−92.33	7.72	−107.75	9.08
method II	−84.59	7.13	−94.93	8.00	−109.89	9.15

Table 4 Prestress loss of tendon W6

Method	One year		Three years		Ten years	
	value (MPa)	rate (%)	value (MPa)	rate (%)	value (MPa)	rate (%)
method I	−75.08	6.33	−84.24	7.1	−95.61	8.06
method II	−79	6.65	−92	7.74	−113	9.51

Table 5 Prestress loss of tendon B7

Method	One year		Three years		Ten years	
	value (MPa)	rate (%)	value (MPa)	rate (%)	value (MPa)	rate (%)
method I	−93.5	8.36	−105.84	9.45	−121.1	10.81
method II	−117.06	10.07	−136.12	11.71	−163.17	14.03

Table 6 Prestress loss of tendon D17

Method	One year		Three years		Ten years	
	value (MPa)	rate (%)	value (MPa)	rate (%)	value (MPa)	rate (%)
method I	−114.17	10.32	−130.80	11.82	−151.42	13.69
method II	−154.54	14.23	−179	16.54	−210.41	19.41

It can be seen from Table 3, Table 4, Table 5 and Table 6 that the loss value of top plate is greater than that of web at pier. This is because the stress of concrete at the top plate is higher than that at the web. The shrinkage and creep effect at the top plate will be greater than that at the web. The loss of prestress calculated by beam element is greater than that by solid element considering the effect of relaxation in prestressed reinforcement on the shrinkage and creep of concrete.

6 Summary

The comparison results of the three prediction models show that the variability of the prediction models is more than 20%. In the prediction of structural shrinkage and creep. It is better to select the appropriate prediction model according to the short-term experimental data, so as to reduce the prediction error. In the absence of data, GL2000 prediction model is recommended.

The finite element analysis of a 60 m prestressed concrete box girder is carried out. The theoretical value is compared with the measured value. The results show that the calculated value by beam element is larger than the measured value. The theoretical value is closest to the measured value by solid element considering the effect of prestressed tendon relaxation on shrinkage and creep.

The following conclusions have been drawn from the detailed analysis of concrete shrinkage and creep effect of a prestressed concrete continuous rigid frame bridge.

The mid-span deflection of the middle span is twice as much as that of the completed bridge in one year. It is three times of that in the ten years after completion of the bridge. The axial displacement of the pier top is also significant. The displacement of the pier top is 104 mm deflecting to mid-span direction when the bridge is completed for 10 years.

The results show that the stress of shrinkage and creep roof gradually decreases from the top of the pier to the middle of the span, while the stress of the bottom plate increases gradually from the top of the pier to the middle of the span. Because of Shrinkage and creep of concrete, the principal compressive stress decreases and the tensile stress increases.

The loss of prestress caused by shrinkage and creep is developing rapidly at the beginning. It gradually slows down after 3 years of completion. The loss value at pier top is less than that at mid span. The value of prestress loss calculated by solid element is less than that calculated by beam element.

References

1. Bazant ZP (2001) Prediction of concrete creep and shrinkage: past, present, and future. Nuclear Eng Des 203(1):27–38
2. Prediction of Creep, Shrinkage and Temperature Effect in Concrete Structure. ACI Committee 209 (1982)
3. Di H (2005) Creep effect theory of concrete structure. The Science Publishing Company, New York City
4. Jian-Ping L (2002) Evaluation of Concrete Shrinkage and Creep Prediction Models. A Thesis for the Degree Master of Science, San Jose State University
5. Gardner NJ (2005) Shrinkage and Creep of Concrete. Hermes Science, London
6. Zhi-hua C (2006) Comparative analysis of concrete creep prediction model. Bridge Constr 5:76–78
7. Wen-sheng, D, Zhi-tao, L, Shao-ping M, Zhao L (2004) Analysis and comparison of prediction models for concrete shrinkage and creep. Bridge Constr 6:13–16 (2004)
8. Shou-hui, C.: Analysis of shrinkage and creep effect of long-span prestressed concrete continuous box girder bridge. Railway Eng 8:15–17 (2009)
9. Zhi-min L (2002) The creep control of pc continuous beam bridge of rail transit. Bridge Constr 3:25–28
10. Fangzhi W (2008) Analysis and field measurement of concrete box girder bridges for shrinkage and creep effects. China Civil Eng J41(1):70–81